

Supporting Information for

Oxygen Vacancy-Rich 2D TiO₂ Nanosheets: A Bridge Toward High Stability and Rapid Hydrogen Storage Kinetics of Nano-Confined MgH₂

Li Ren^{1,2,3}, Wen Zhu¹, Yinghui Li¹, Xi Lin¹, Hao Xu¹, Fengzhan Sun¹, Chong Lu⁴, and Jianxin Zou^{1,2,3*}

¹National Engineering Research Center of Light Alloys Net Forming & State Key Laboratory of Metal Matrix Composites, Shanghai Jiao Tong University, Shanghai, 200240, PR China

²Shanghai Engineering Research Center of Mg Materials and Applications & School of Materials Science and Engineering, Shanghai Jiao Tong University, Shanghai, 200240, PR China

³Center of Hydrogen Science, Shanghai Jiao Tong University, Shanghai, 200240, PR China

⁴Instrumental Analysis Center of SJTU, Shanghai Jiao Tong University, Shanghai, 200240, PR China

*Corresponding author: E-mail: zoujx@sjtu.edu.cn; Tel: +86 21 54742381; Fax: +86 21 34203730

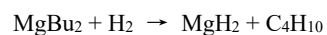
Supplementary Figures and Tables

Table S1 Summary of the precursors used for the synthesis of MgH₂/TiO₂ heterostructure

Samples	Amount of MgBu ₂ (mL)	Amount of TiO ₂ (mg)
blank MgH ₂	1.8	0
40MgH ₂ /TiO ₂	0.8	30
50MgH ₂ /TiO ₂	1.2	30
60MgH ₂ /TiO ₂	1.8	30
70MgH ₂ /TiO ₂	2.7	30
80MgH ₂ /TiO ₂	4.6	30

Note:

The amounts of MgH₂ in the prepared MgH₂/TiO₂ heterostructures are calculated according to the formula below:



For example, 1.8 mL of MgBu₂ (1.8 mmol) can be hydrogenated to obtain 46.8 mg of MgH₂. Therefore, the weight percentage of MgH₂ in the MgH₂/TiO₂ heterostructure (m(TiO₂) = 30 mg) is calculated to be about 60 wt.% (46.8 mg/(30+46.8) mg).

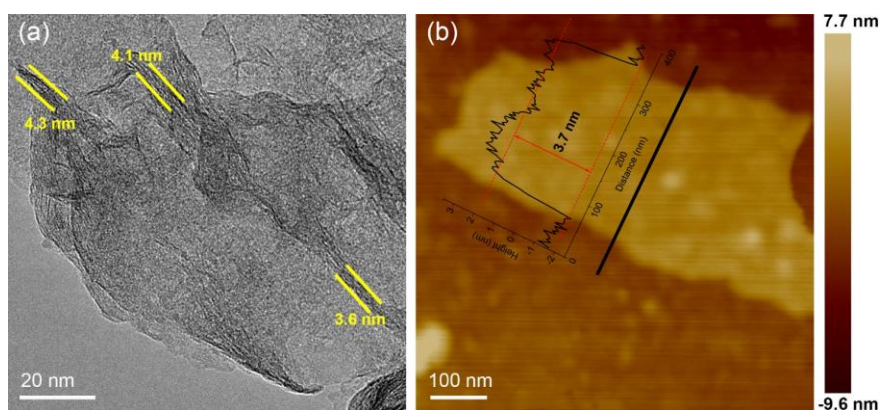


Fig. S1 **a** Typical TEM image showing the edge configuration of 2D TiO₂ NS. **b** AFM image demonstrating the thicknesses of a 2D TiO₂ nanosheet to be ~3.7 nm

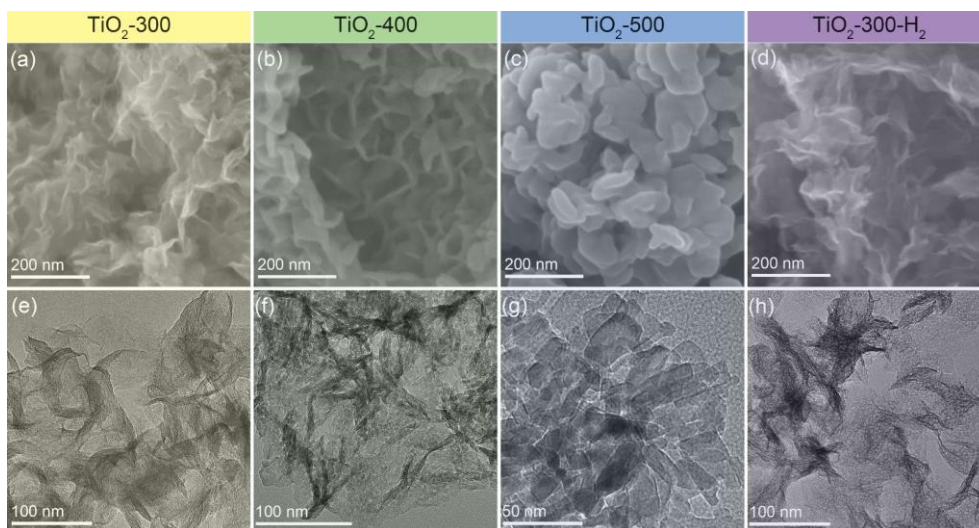


Fig. S2 Typical SEM images **a-d** and TEM images **e-h** of TiO₂ NS annealed at different temperatures

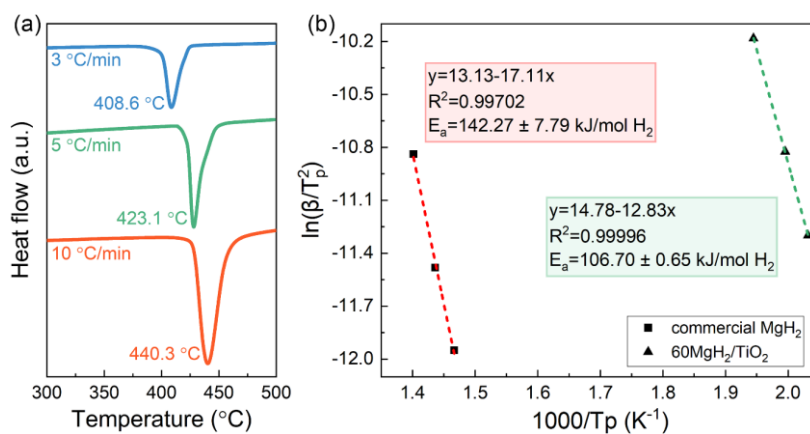


Fig. S3 **a** DSC curves of the commercial MgH₂. **b** Kissinger's plots of 60MgH₂/TiO₂ and commercial MgH₂

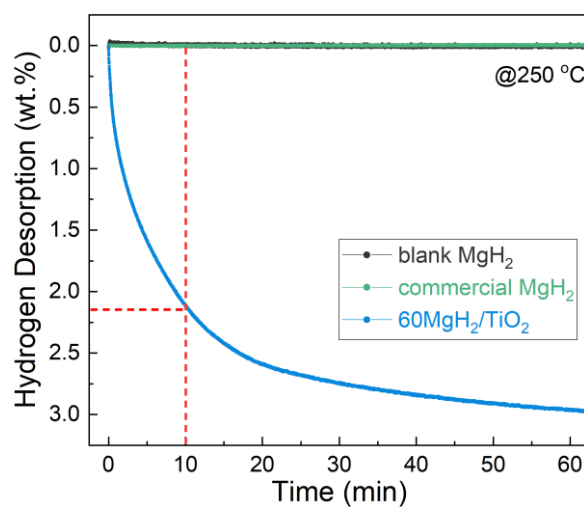


Fig. S4 The comparison of isothermal desorption behaviors of blank MgH₂, commercial MgH₂, and 60MgH₂/TiO₂

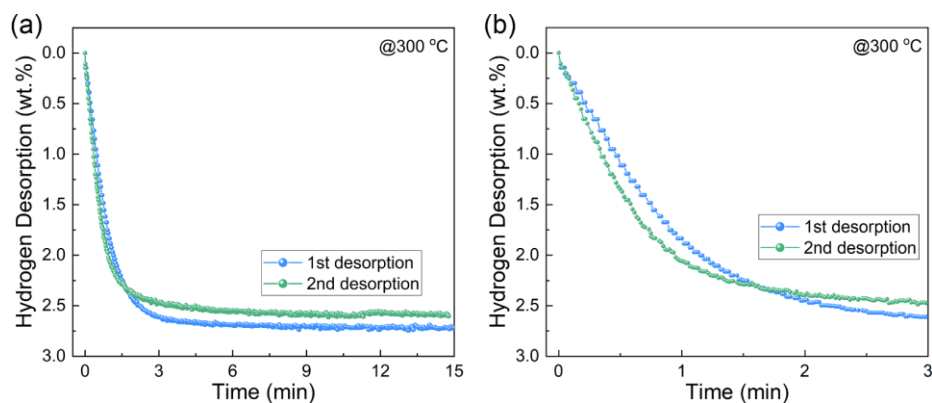


Fig. S5 **a** The comparison of isothermal desorption behaviors of 60MgH₂/TiO₂ in the first two cycles at 300 °C and **b** the corresponding enlarged view for the first three minutes

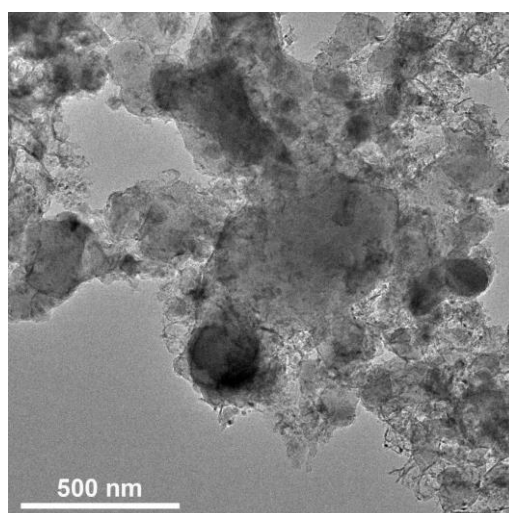


Fig. S6 Typical TEM image of blank MgH₂ synthesized without TiO₂ NS after several de/re-hydrogenation cycles

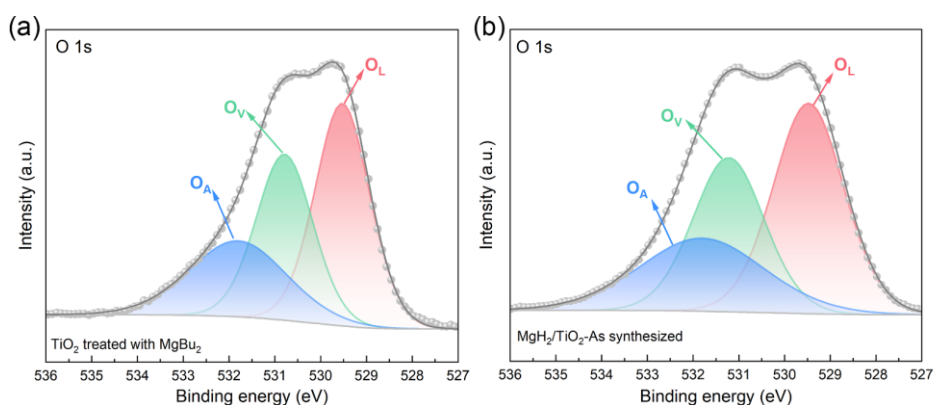


Fig. S7 O 1s XPS spectra of **a** the TiO₂ nanosheets treated with MgBu₂ and **b** the as-synthesized MgH₂/TiO₂ heterostructure (O_A: Adsorbed oxygen; O_V: Oxygen vacancy; O_L: Lattice oxygen)

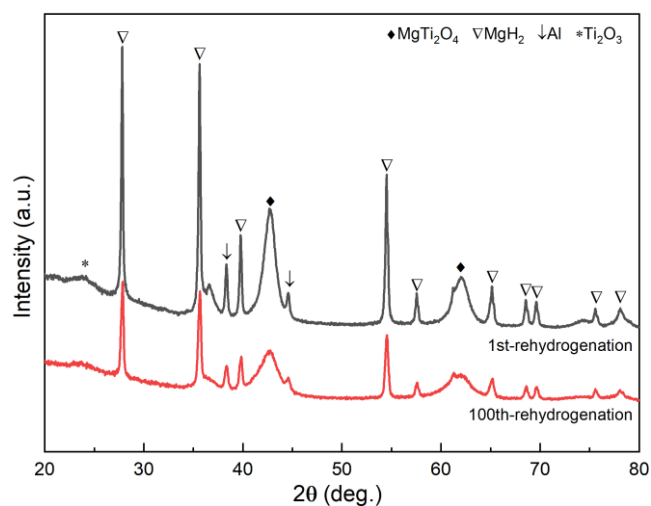


Fig. S8 XRD patterns of the re-hydrogenated MgH₂/TiO₂ heterostructure after 1 de/re-hydrogenation cycle and 100 de/re-hydrogenation cycles

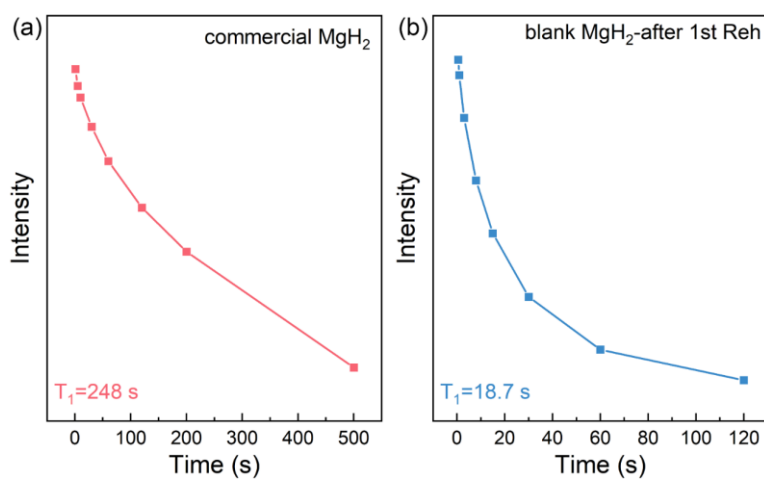


Fig. S9 NMR spin-lattice relaxation curves of **a** commercial MgH₂ and **b** blank MgH₂ after the 1st re-hydrogenation

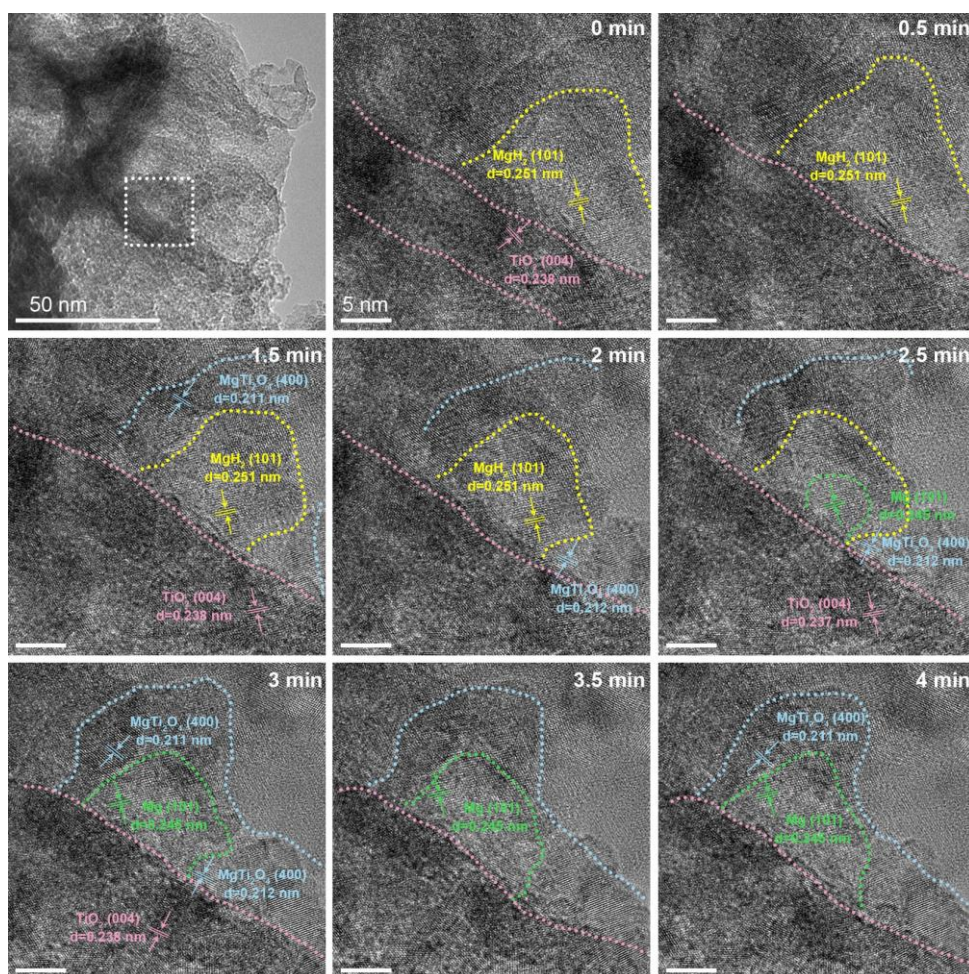


Fig. S10 Typical TEM and HRTEM images of the hydrogenated $\text{MgH}_2/\text{TiO}_2$ composites under electron beam radiation during the hydrogen desorption process

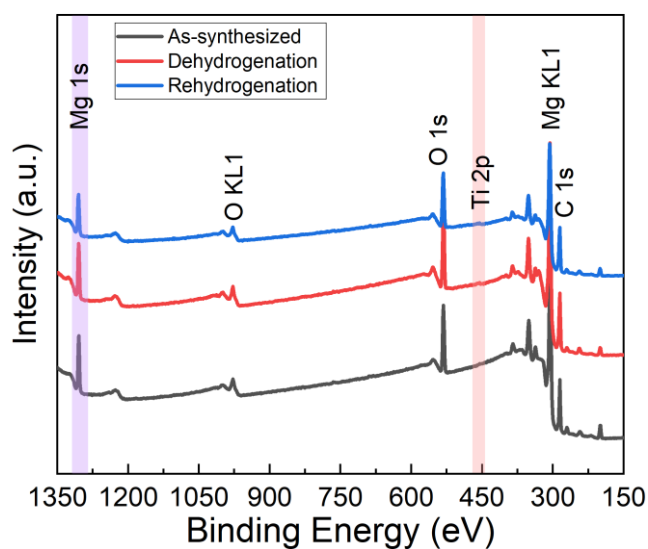


Fig. S11 XPS spectra of the $\text{MgH}_2/\text{TiO}_2$ heterostructure at different states

Table S2 Comparison of hydrogen storage performances of MgH₂/TiO₂ heterostructure in the present work with other MgH₂ based systems

Scaffolds /catalysts ^{a)}	Loading capacity (wt.%)	System gravimetric capacity (wt.%)	T _{onset} (°C) (hydrogen desorption)	T _{peak} (°C) (heating rate: 5 °C min ⁻¹)	Initial dehydrogenation rate at 300 °C (wt% min ⁻¹)	Refs
Graphene	60	4.5	250	340	0.7	[S1]
CMK-3	40-60	2.4-3.7	250	300-260	None	[S2]
Carbon aerogels	10	1.5 ^{b)}	220	280	None	[S3]
TiO ₂ @C ^{a)}	90	6.5	205	259 (6 °C min ⁻¹)	1.12	[S4]
Carbon aerogels	18.2	1.14	200	385 (3.6 °C min ⁻¹)	None	[S5]
3D TiO ₂ ^{a)}	95	6.7	199.2	245.4	None	[S6]
2D TiO ₂ (B) ^{a)}	90	6.29	200	227.6	None	[S7]
BCNT	78	5.79	237.5	276.7	0.75	[S8]
TiO ₂ @Gr ^{a)}	90	6.5	270	290 (10 °C min ⁻¹)	0.38	[S9]
CoS	60	3.1	297	314	0.255	[S10]
Ni-MOF	50	2.7	314.5	330.4	None	[S11]
TiO ₂	60	3.4	180	228.7	2.116	This work

Note:

^{a)} The synthesis method is high-energy ball milling.

^{b)} Calculation of the gravimetric capacity does not include the weight of the scaffold.

Supplementary References

- [S1] Y. Huang, G. Xia, J. Chen, B. Zhang, Q. Li, X. Yu, One-step uniform growth of magnesium hydride nanoparticles on graphene. *Prog. Nat. Sci.* **27**(1), 81-87 (2017). <https://doi.org/10.1016/j.pnsc.2016.12.015>
- [S2] M. Konarova, A. Tanksale, J. Norberto Beltramini, G. Qing Lu, Effects of nano-confinement on the hydrogen desorption properties of MgH₂. *Nano Energy* **2**(1), 98-104 (2013). <https://doi.org/10.1016/j.nanoen.2012.07.024>
- [S3] Y. S. Au, M. K. Obbink, S. Srinivasan, P. C. M. M. Magusin, K. P. de Jong, P. E. de Jongh, The Size Dependence of Hydrogen Mobility and Sorption Kinetics for Carbon-Supported MgH₂ Particles. *Adv. Funct. Mater.* **24**(23), 3604-3611 (2014). <https://doi.org/10.1002/adfm.201304060>
- [S4] X. Zhang, Z. Leng, M. Gao, J. Hu, F. Du, J. Yao, H. Pan, Y. Liu, Enhanced hydrogen storage properties of MgH₂ catalyzed with carbon-supported nanocrystalline TiO₂. *J. Power Sources* **398**, 183-192 (2018). <https://doi.org/10.1016/j.jpowsour.2018.07.072>
- [S5] T. K. Nielsen, K. Manickam, M. Hirscher, F. Besenbacher, T. R. Jensen, Confinement of MgH₂ Nanoclusters within Nanoporous Aerogel Scaffold Materials. *ACS Nano* **3**(11), 3521-3528 (2009). <https://doi.org/10.1021/nn901072w>
- [S6] M. Zhang, X. Xiao, B. Luo, M. Liu, M. Chen, L. Chen, Superior de/hydrogenation performances of MgH₂ catalyzed by 3D flower-like TiO₂@C

- nanostructures. *J. Energy Chem.* **46**, 191-198 (2020). <https://doi.org/10.1016/j.jechem.2019.11.010>
- [S7] M. Chen, X. Z. Xiao, M. Zhang, J. F. Mao, J. G. Zheng, M. J. Liu, X. C. Wang, L. X. Chen, Insights into 2D graphene-like TiO₂ (B) nanosheets as highly efficient catalyst for improved low-temperature hydrogen storage properties of MgH₂. *Mater. Today Energy* **16**, 100411 (2020). <https://doi.org/10.1016/j.mtener.2020.100411>
- [S8] M. Liu, S. Zhao, X. Xiao, M. Chen, C. Sun, Z. Yao, Z. Hu, L. Chen, Novel 1D carbon nanotubes uniformly wrapped nanoscale MgH₂ for efficient hydrogen storage cycling performances with extreme high gravimetric and volumetric capacities. *Nano Energy* **61**, 540-549 (2019). <https://doi.org/10.1016/j.nanoen.2019.04.094>
- [S9] S. K. Verma, A. Bhatnagar, V. Shukla, P. K. Soni, A. P. Pandey, T. P. Yadav, O. N. Srivastava, Multiple improvements of hydrogen sorption and their mechanism for MgH₂ catalyzed through TiH₂@Gr. *Int. J. Hydrog. Energy* **45**(38), 19516-19530 (2020). <https://doi.org/10.1016/j.ijhydene.2020.05.031>
- [S10] Z. Ma, S. Panda, Q. Zhang, F. Sun, D. Khan, W. Ding, J. Zou, Improving hydrogen sorption performances of MgH₂ through nanoconfinement in a mesoporous CoS nano-boxes scaffold. *Chem. Eng. J.* **406**, 126790 (2021). <https://doi.org/10.1016/j.cej.2020.126790>
- [S11] Z. Ma, Q. Zhang, S. Panda, W. Zhu, F. Sun, D. Khan, J. Dong, W. Ding, J. Zou, In situ catalyzed and nanoconfined magnesium hydride nanocrystals in a Ni-MOF scaffold for hydrogen storage. *Sustain. Energy Fuels* **4**(9), 4694-4703 (2020). <https://doi.org/10.1039/D0SE00818D>